

Formation of dwarf ellipticals and dwarf irregular galaxies by interaction of giant galaxies under environmental influence

Tanuka Chattopadhyay^a, Suma Debsarma^a, Pradip Karmakar^a, Emmanuel Davoust^b

^a*Department of Applied Mathematics, Calcutta University, 92 A.P.C Road, Calcutta 700009*

^b*Institut de Recherche en Astrophysique et Planétologie, Université de Toulouse/CNRS, 14 Avenue Edouard Belin, 31400 Toulouse, France*

Abstract

A model is proposed for the formation of gas-rich dwarf irregular galaxies and gas-poor, rotating dwarf elliptical galaxies following the interaction between two giant galaxies as a function of space density. The formation of dwarf galaxies is considered to depend on a random variable, the tidal index Θ , an environmental parameter defined by Karachentsev et al. (2004), such that for $\Theta < 0$ the formation of dwarf irregular galaxy is assured whereas for $\Theta > 0$ the formation of dwarf ellipticals is preferred. It is found that for particular ranges of the interactive parameters the model predictions are in good agreement with the observed number density of the different galaxy types as a function of space density in four clusters of galaxies. This supports the fact that galaxy interactions do not all necessarily give rise to the formation of either dwarf irregulars or dwarf ellipticals. It is also shown that the formation of dwarf irregulars at high densities is much lower than that of dwarf ellipticals, and that the formation of the latter reaches a maximum at a particular space density, unlike the former. This

Email addresses: tanuka@iucaa.ernet.in (Tanuka Chattopadhyay), debsarma@rediffmail.com (Suma Debsarma), edavoust@irap.omp.eu (Emmanuel Davoust)

suggests that at high densities many dwarf irregulars are stripped of their gaseous envelopes to become dwarf elliptical.

Keywords:

dwarf galaxies, data analysis, statistical

1. Introduction

Dwarf galaxies are small, low-luminosity and low-metallicity galaxies. In spite of their vast majority over other morphological types (Sandage & Binggeli 1984; Ferguson & Binggeli 1994; Mateo 1998) their formation scenario is still far from understood. Giant galaxies generally form either through the gravitational collapse of a huge protogalactic gas cloud (Larson 1974; Dekel & Silk 1986; White & Frenk 1991; Frenk et al. 1996; Kauffmann et al. 1997), by merger of two or more disc galaxies (Toomre 1977; Ashmann & Zepf 1992; Zepf et al. 2000), by multiphase dissipative collapse (Forbes et al. 1997), by dissipationless merger model, or by accretion and in situ hierarchical merging (Côté et al. 1998; Mondal et al. 2008; Chattopadhyay et al. 2009). Dwarf galaxies, on the other hand, occupy a separate region in the Fundamental Plane (Kormendy 1985; Chattopadhyay et al. 2012; Chattopadhyay & Karmakar 2013), which suggests that they have a different formation mechanism.

Some dwarf galaxies might be formed by galaxy collisions because dwarf irregular galaxies (hereafter dIrrs) have been found in the tidal tail of interacting galaxies (Schweizer 1982; Bergvall & Johansson 1985; Mirabel et al. 1991; Braine et al. 2000; Weilbacher et al. 2000; Ferreira et al. 2005; Mendes de Oliverira et al. 2000; Mundell et al. 2004; Sheen et al. 2009; Kaviraj et al. 2012). The formation of tidal dwarf galaxies has also been demonstrated by numerical simulations (Barnes & Hernquist 1992; Bournaud & Duc 2006; Dabringhausen & Kroupa 2013). The formation of tidal dwarf galaxies from stripped gas has been reviewed by Bournaud (2010). Kroupa (2012) has shown that the existence of two types of dwarf galaxies (with or without dark matter) is incompatible with the current standard model of cosmology. The

formation of ultra-compact dwarf galaxies (which have masses in the range $10^6 M_\odot$ to $10^8 M_\odot$ and radii 10 pc -100 pc) is a different issue (Dabringhausen et al. 2008; Chattopadhyay et al. 2012; Chattopadhyay & Karmakar 2013).

The formation of dwarf ellipticals (hereafter dEs), on the other hand, is probably related to early-type galaxies (E or S0), because the frequencies of dEs and giant early types are increasing functions of space density (Binggeli et al. 1990; Ferguson & Binggeli 1994). Also van Zee et al. (2004) have observed 16 dEs in the Virgo cluster and found that they are similar to dIrrs in rotation amplitude and luminosity. These observations suggest that some cluster dEs may be formed when the neutral gaseous medium of dIrrs is stripped under the influence of some environmental factor (Dunn 2010). Investigating the formation of dwarf galaxies as a result of giant galaxy interaction and the condition under which dIrrs and dEs are formed is thus now a priority.

In the present paper we develop a numerical statistical simulation model for the formation of dIrr and dE galaxies along with giant galaxies as a function of increasing space density. This is a more extended version of the galaxy interaction models of Silk & Norman (1981) and Okazaki & Taniguchi (2000). We have considered a random production of dIrr and dE galaxies during each interaction on the basis of an environmental parameter, the tidal index Θ (Karachentsev et al. 2004). We describe the model in section 2, the observations are presented in section 3, and the results and interpretations are given in section 4.

2. Model

The present model is based on the scenario of fragmentation and hierarchical clustering scheme of galaxy formation. According to this scenario, the primordial density fluctuation at recombination is $\delta\rho/\rho \sim (M/M_0)^{-\alpha}$ (Efstathiou 1979), where $\alpha \sim 1/2$ for (for $\Omega \sim 1$) or $\alpha \sim 1/3$ (for $\Omega \sim 0.1$). Hence $M_o \sim 10^{14.9-3/\alpha} \Omega^{1-1/\alpha} h^{-1}$ ($h = H_o/50 \text{ km s}^{-1} \text{ Mpc}^{-1}$). So a primordial spectrum of isothermal density fluctuation in the

early universe could form bound clouds of mass M_0 at $z \sim 1000$ i.e. $M_0 \sim 10^8 M_\odot (\Omega \sim 0.1)$ to $10^9 M_\odot (\Omega \sim 1)$. Such clouds can survive for times longer compared to their collapse time scales (SN81). These gas clouds are clustered gravitationally forming gas rich protogalaxies at a late epoch ($z \leq 10$) (Peebles 1974 ; Davis & Peebles 1977; Gott et al. 1979). The gas clouds that form protogalaxies interact dissipatively and dissipation leads to the formation of the luminous parts of galaxies. The dark material or the parent material of these clouds play an important role in forming galaxy clusters and haloes. White and Rees (1978) have shown that the growth of density fluctuations on larger scales can be described by a spectrum $\delta\rho/\rho = (M/M_i)^{1/2-n/6} (t/t_i)^{2/3}$ which leads to $M/M_i \sim (R/R_i)^{6/(n+5)}$ in an Einstein-de-Sitter Universe ($\Omega \sim 1$). This leads to $M_i \sim 5 \times 10^{14} (1+z_i)^{-2} M_\odot$ and $R_i \sim R_0 (1+z_i)^{-5/3}$ for an observed galaxy correlation function and $n=0$. $z_i (\leq 10)$ is the epoch of galaxy clustering. The protogalaxies ultimately form clusters of galaxies at $z \leq 10$. Hence the onset of galaxy clustering is generally considered at $z \sim 5 - 10$. During the initial phase of galaxy clustering many collisions among these protogalaxies will occur and those result in mergers.

Dressler(1980) has observed the fraction of galaxies of various morphological types as a function of local density in rich clusters. For instance in small groups and other low density regions, the fraction of bright galaxies which are spiral, is around 80 %, with about 20% S0s and very few ellipticals. Moving inward from the outskirts of a cluster, the fraction of spirals decreases steadily while the S0 fraction rises steadily but is rapidly caught up by the elliptical fraction once high densities are reached.

Hence following the study of Dressler(1980) we have assumed that initially at the onset of the galaxy clustering epoch (lowest space density) all the galaxies are protospirals. A model of protogalaxy interaction was first introduced by Silk & Norman(1981) and it reproduced the observed fraction of galaxies of various morphological types as a function of logarithm of the ratio of S0s to spiral. This ratio is proportional to the space density. Subsequently Okazaki & Taniguchi (2001) have also

considered merger of such protogalaxies and in addition each interaction in their model was accompanied with a production of dwarf galaxy whose morphology was not specified. All the previous models considered that initially at the epoch of galaxy clustering all the protogalaxies were protospirals.

The present model, like the one of Okazaki & Taniguchi (2001), considers the production of a dwarf galaxy as a result of protogalaxy interaction, but each time it is produced its morphology is determined on the basis of an environmental parameter Θ which is a random variable defined by Karachentsev & Makarov (1988). Θ describes the local mass density around a galaxy i as $\Theta_i = \max[\log(M_k/D_{ik})^3] + C, i = 1, 2, \dots, N$ where M_k is the total mass of any neighbouring galaxy separated from the considered galaxy by distance D_{ik} . In a previous paper (Chattopadhyay et al. 2010) we classified dwarf galaxies on the basis of several parameters and found two groups, one dominated by dIrrs and the other by dEs, and for these two groups the average value of Θ was negative and positive, respectively. The observed values of Θ , taken from Karachentsev et al.(2004), are given in Table 1 along with galaxy names and morphological indices T.

The distribution of Θ has been successfully fitted by a Gamma distribution (Anderson Darling value, which is a measure of goodness of fit, is 0.65). Since the Gamma distribution is valid for positive values only we have used a coordinate transformation $Y = X+3$ to make all observed $y_i \geq 0$. Here X and Y are two random variables. In particular X stands for Θ . y_i ($i = 1, 2, \dots$) are the observed values of Y found by the above translation over all observed values of Θ . Then after fitting the distribution we used the back substitution $X = Y - 3$ for getting the original values of the variables. Now for each iteration we have generated Θ randomly (See Appendix 1) from the Gamma distribution (Fig. 1). If $\Theta < 0$ we assume that a dIrr galaxy has been produced and if $\Theta > 0$, a dE has been produced.

Hence the present model includes the formation of both dIrrs and dEs as a result of tidal interactions between giant galaxies, either Spirals, Lenticulars or both. This is warranted by numerous observational studies of dwarf galaxies found in interacting or merging giant galaxies (Bergvall & Johansson 1985; Mirabel et al. 1991; Hibbard & Higdon 2001; Delgado-Donate et al. 2003; Knierman et al. 2003; Mundell et al. 2004; Allam et al. 2007; Duc et al 2007; Kaviraj et al. 2012). We consider the production of dEs and dIrrs separately, rather than that of dwarf galaxies in general. Both types of dwarf galaxies can be produced in each interaction and the production of either type is random. Our model also includes the production of ellipticals and/or of lenticulars. The case of forming an elliptical in the merger of two spiral galaxies (Ashman & Zepf 1992; Zepf et al 2000) had not been considered in the previous papers on this subject. The scheme of interaction assumes that at each interaction a dwarf galaxy is produced, and its type depends on Θ which is drawn randomly. This scheme is summarized in Table 2. For a draw of any random value of Θ , if $\Theta > 0$ we assume that k_1 dEs are produced and if $\Theta < 0$ k_1' dIrrs are produced. Since the production of different types of dwarfs is random we have used a 'slash' in each interaction of the merger tree. In Table 2, the parameters a, b, c, d, and e are the probabilities with which the impact between protogalaxies occur and are called impact parameters. Based on the scheme of Table 2, the kinetic equations for the evolution of each morphological type reduces to,

$$\frac{1}{\gamma} \frac{dn_{Sp}}{dt} = -2a n_{Sp}^2 - n_{S0}n_{Sp} \quad (1)$$

$$\frac{1}{\gamma} \frac{dn_{S0}}{dt} = a n_{Sp}^2 - b n_{S0}n_{Sp} - d n_{S0}^2 + e n_{S0}n_{Sp} \quad (2)$$

$$\frac{1}{\gamma} \frac{dn_E}{dt} = (1 - a) n_{Sp}^2 + b n_{S0}n_{Sp} + c n_{S0}n_{Sp} + d n_{S0}^2 \quad (3)$$

$$\frac{1}{\gamma} \frac{dn_{dIrr}}{dt} = [k'_1 a + k'_2 (1-a)] n_{Sp}^2 + [k'_3 b + k'_4 c + k'_5 \{1 - (b+c+e)\}] n_{S0} n_{Sp} + [d k'_6 + (1-d) k'_7] n_{S0}^2 \quad (4)$$

$$\frac{1}{\gamma} \frac{dn_{dE}}{dt} = [k_1 a + k_2 (1-a)] n_{Sp}^2 + [k_3 b + k_4 c + k_5 \{1 - (b+c+e)\}] n_{S0} n_{Sp} + [d k_6 + (1-d) k_7] n_{S0}^2 \quad (5)$$

where $n_{Sp}, n_{S0}, n_E, n_{dIrr}, n_{dE}$ are the

number densities of Spirals (Sps), lenticulars (S0s), ellipticals (Es), dIrrs and dEs respectively, γ is the mean collision rate and k_i ($i = 1-7$) and k'_i ($i = 1 - 7$) are the numbers of respective dEs and dIrrs formed in each collision. The differential equations were constructed from the merger tree. For example, equation (2) gives the change in the number density of S0s with time. S0s decrease in number with probability b when one Sp and one S0 interact and with probability d when two S0 galaxies interact. The number density is increased with probability a when two Sps interact, and with probability e when one S0 and one Sp interact. Similarly the remaining equations follow. Concerning dn_{Sp}/dt we have assumed that the decrease in spiral galaxies is dominated by the production of S0s more than by that of Es (Dressler et al. 1997; Ellis et al. 1997; Ghigna et al. 1998; van Dokkum 2002). In order to solve equations (1) to (5), we introduce the variable $x = n_{Sp}/n_{S0}$ which decreases monotonically with increasing galaxy density (Silk & Norman 1981 ; Okazaki & Taniguchi 2000). Then we obtain the implicit solution as,

$$\frac{n_{Sp}}{n_0} = \left[\left\{ \frac{ax^2}{ax^2 + (2a + e - b)x + (1 - d)} \right\}^{\frac{1}{2(1-a)}} \right] \cdot \exp\left[\frac{(2a + e - b)d}{(1 - d)a\Delta} \left(\tan^{-1} \left\{ \frac{2ax + (2a + e - b)}{2a\Delta} \right\} - \frac{\pi}{2} \right) \right] \quad (6)$$

$$n_{S0} = \frac{n_{Sp}}{x} \quad (7)$$

$$n_E = \int_x^\infty \frac{n_{Sp}\{(1-a)x^2 + (b+c)x + d\}}{x^2\{ax^2 + (2a+e-b)x + (1-d)\}} dx \quad (8)$$

$$n_{dE} = \int_x^\infty \frac{(Ax^2 + Bx + C)n_{Sp}}{x^2\{ax^2 + (2a+e-b)x + (1-d)\}} dx \quad (9)$$

$$n_{dIrr} = \int_x^\infty \frac{(A'x^2 + B'x + C')n_{Sp}}{x^2\{ax^2 + (2a+e-b)x + (1-d)\}} dx \quad (10)$$

where $A = k_1a + k_2(1-a)$,
 $B = k_3b + k_4c + k_5\{1 - (b+c+e)\}$ and
 $C = dk_6 + (1-d)k_7$

and A', B', C' are identical with A, B and C respectively, except for replacing k_i (i= 1-7) by k'_i (i= 1-7).

$$\Delta^2 = \frac{(1-d)}{a} - \left\{ \frac{(2a+e-b)}{2a} \right\}^2.$$

Since $\Delta^2 > 0$, $\frac{(b-e)}{2} < a < 1$ and also

we have $0 \leq a \leq 1$, $0 \leq b+c+e \leq 1$, $0 \leq d \leq 1$.

(see the Appendix 2 for the actual derivation of equations (6) to (10)).

We have mentioned that initially all galaxies are assumed to be spiral galaxies and their initial number density is n_0 . Initially we assume $k_i = k'_i$ (i = 1-7) but then for each increment Δx of x we take decrements of k_i and k'_i as Δk_i and $\Delta k'_i$, if corresponding to Θ a dE or dIrr galaxy is formed, otherwise there is no decrement in k_i or k'_i (i =1-7) respectively. Our objective is to find plausible ranges of the impact parameters and values of k_i and k'_i (i= 1-7) for which the computed number densities of galaxies of different morphological types as a function of $\log(1/x)$ are consistent with the number densities of the observed ones i.e. the χ^2 goodness of fit value between observed and simulated values are small enough ($\chi^2 < 1$ with high p-value).

3. Data

We have used three data sets, which are described in Table 3. The first one consists of one sample in the Virgo cluster and four in Coma (Michard & Andreon 2008). Coma0 is the full sample of Coma galaxies, whereas Coma1, 2 and 3 consist of galaxies at increasing distances from the cluster center. The second one is a sample in the Centaurus cluster (Jergen & Dressler 1997). In this sample, irregular galaxies having magnitudes $M_B \geq -10$ are considered as dIrrs. The last sample is that of 2096 galaxies in the Virgo cluster (Binggeli et al. 1985). In this sample, irregular galaxies with magnitudes $M_B \geq -16$ are considered as dIrrs. In Table 3, the parameter x is the ratio of spirals to lenticulars defined above.

4. Results and discussions

In order to find the best model we minimize the sum of squares of the deviations between predicted and observed number of galaxies of various morphological types weighted by the predicted number of galaxies i.e. $\sum_{i=1}^5 \sum_{j=1}^N \frac{(n_{pred} - n_{obs})_{i,j}^2}{n_{pred}} = \chi^2$ where i stands for the five morphological types (viz. Sp, S0, E, dE, dIrr) and j stands for the data points of groups and clusters given in Table 3, N is the total number of galaxies of each type. n_{pred} (found from equations (6)-(10)) is the number of predicted galaxies and n_{obs} (found from Table 3) is the number of observed galaxies. Table 4 shows the best ranges of impact parameters a, b, c, d, e and values of k_i and k'_i ($i=1-7$) for which χ^2 is small enough together with a high level of significance (characterized by p-value, $p=0.995$).

Our simulations show that the fraction of spiral galaxies decreases very slowly up to $\log(1/x) = -0.5$ and after that point the fall is almost exponential and the χ^2 goodness of fit value with an exponential curve gives a very small value of $\chi^2 \sim 0.12$ for $-0.5 < \log(1/x) \leq 2$. We remind the reader that $\log(1/x)$ increases monotonically with increasing space density. The fractions of E and S0 galaxies have moderate maxima around $\log(1/x) = -0.5$ and 0 respectively.

The maximum of $\log(1/x)$ for Es occurs at a lower space density than that of S0s. This must be due to the formation process of the latter, by gas stripping in Spirals, which is favored by high density environments. The peak for S0 galaxies at $\log(1/x) = 0$ is close to the value found by Okazaki & Taniguchi (2000), but the peak for ellipticals is at a lower value than the one found by them.

In our simulations, the fraction of dE galaxies has a pronounced peak at $\log(1/x) \simeq 0$ and it decreases at higher values of $\log(1/x)$, i.e. as $\log(1/x)$ tends to 2 the fraction is close to zero (Fig.2, green solid line). The fraction of dIrrs is much smaller than that of dEs and it is also a decreasing function of space density. The low number of dIrrs compared to dEs at medium densities may be due to the fact that gas stripping from a large number of dIrrs by neighboring galaxies leads to the formation of dEs (van Zee et al. 2004). The fall in the fraction of dEs at still higher densities may be due to the decreasing fraction of spiral galaxies in the high-density regime taking part in the interaction. There are also very few dwarfs in regions of low space density. This is consistent with observations (Yahil et al.1998; Shanks et al 2001; Mathews et al. 2004).

The observed fraction of galaxies of various morphological types is in the range $-0.5 < \log(1/x) < 0.5$ (see Fig.2 and Table 3). Ann (2007) observed various dwarf galaxies in the local Universe and derived the local density (ρ) by calculating the mass of galaxies with a projected distance of 1 Mpc and a line of sight velocity difference less than 500 km/s assuming constant M/L. Ann (2007) plotted the fraction of 'dE,N', Im, dS0 and dE versus $\log(\rho)$ and found that the majority of dE galaxies are located in the overdense regions, with a peak around $\log(\rho) \sim 1$. This is similar to our result that dE occurs in dense regions (Fig.2) i.e. in clusters of galaxies rather than in the field.

We now turn to the number of galaxies of various morphological types produced in our simulations. dEs and dIrrs have their maxima around $k_i = 2$ and $k'_i = 1$, ($i = 1-7$) respectively from best fitting.

This is almost consistent with the observations of dwarf galaxies in individual galaxy interaction (Table 5) i.e. the maximum values of k_i and k'_i ($i = 1-7$) in Fig.3 are 2 and 1 which are close to the values 1/2/3 for most of the observations in Table 5. It is to be mentioned that the type of dwarf galaxies has not been specified in Table 5. In the highest density regime (viz. $\log(1/x)$ in the range 0 - 2), the formation rates of dwarf galaxies of both types in individual interaction are roughly constant (viz. $k_i \sim 2$ for dEs and $k'_i \sim 1$ for dIrrs).

The curve for k_1 (in magenta) runs higher than the other curves in the top right graph of Fig.3, whereas the curve for k'_4 (in cyan) runs higher than the other ones in the bottom right graph of Fig.3. Now k_1 is the number of dEs formed from Sp+Sp interaction (viz Table 2) and k'_4 is the number of dIrrs formed from Sp+S0 interaction. Hence the formation of dIrrs is preferred in Sp+S0 interaction compared to Sp+Sp for dEs. Kaviraj et al.(2012) have performed a statistical observational study of tidal dwarf populations using a homogeneous catalogue of galaxy mergers from SDSS. They found that mergers producing tidal dwarfs involve two progenitor spirals in 95% of the cases and at least one progenitor spiral in the remaining cases. The fraction of tidal dwarfs where both parents are of early type is less than 2%. These results are almost consistent with the results in the present paper.

The main innovation of the present model, compared to those of Silk & Norman (1981) and Okazaki & Taniguchi (2000) is that we are able to trace separately the formation of dEs and dIrrs as a function of increasing space density using the environmental parameter Θ . This is important because the formation of dE or dIrr galaxies constrained by the tidal environment remained controversial. It has been claimed that dEs are transformed from dIrrs when enough gas is expelled as a result of tidal influence by neighbouring galaxies (van Zee et al. 2004; Dunn 2010). Hence the question remained how these two types of dwarf galaxies are formed. We have incorporated the above idea in the present model

by assuming that the formation of dEs or dIrrs depends on a random variable Θ (Karachentsev et al. 2004). We indeed found in an earlier paper (Chattopadhyay et al. 2010) that dE galaxy formation is preferred when $\Theta > 0$ and that of dIrrs when $\Theta < 0$. We also considered values of $\log(1/x)$ up to 2, thus reflecting the proper trend of number density of the different galaxy types as a function of increasing space density, whereas Okazaki & Taniguchi (2000) only considered values of $\log(1/x)$ up to 1.

In conclusion, assuming that most of the present-day dwarf galaxies originate from galaxy interactions, we have been able to find model parameters (a, b, c, d, e) which give results in agreement with the observations in different environments. This suggests that most present-day dwarfs were formed in protogalaxy interactions, and that they are not building blocks of the hierarchical formation of galaxies.

5. Acknowledgements

T. C. thanks DST, India for supporting her a Major Research Grant. The authors are very grateful for the various points suggested by the referee for improving the work. The authors are also grateful to A.K. Chattopadhyay for his fruitful suggestions.

6. Appendix 1: Generation of random sample from Gamma distribution

The probability density function (pdf) of the Gamma distribution of a random variable X (here Θ) is

$$f(x; k, \theta) = \frac{x^{k-1} e^{-\frac{x}{\theta}}}{\theta^k \Gamma^k}, \text{ for } x > 0, \theta > 0$$

where k is the shape parameter and $1/\theta$ is its rate

parameter. Now for a given pdf $f(x)$, the cumulative distribution function (cdf), $F(x) = P(0 \leq X \leq x) = \int_0^x f(x) dx$.

where $F(x)$ is a random number r and $0 < r, 1$. Then $x = F^{-1}(r)$ generates a sample value x of X for a randomly chosen r .

Since the Gamma distribution is one of the many distributions from which it is difficult or even impossible to directly simulate by the above inverse transform, we use the Accept-Reject method by which samples can be generated from the target density $f(x)$ through

another density $g(x)$, known as the instrumental density.

If f is the density of interest (which is Gamma in our case) known as target density on an arbitrary space we can write $f(x) = \int_0^{f(x)} dr$. Thus f appears as the marginal density of the joint distribution $(x, R) \sim \text{uniform}\{(x, r), 0 < r < f(x)\}$. Hence simulating $X \sim f(x)$ is equivalent to simulating $(X, R) \sim \text{uniform}\{(x, r), 0 < r < f(x)\}$. As the simulation of the uniform pair (X, R) is often not straightforward we use the following simplification (Robert & Casella 2004) Let $X \sim f(x)$ and let $g(x)$ be a density function that satisfies $f(x) \leq Mg(x)$ for some constant $M \geq 1$. Then to simulate $x \sim f$ it is sufficient to generate $Y \sim g(y)$ and $R|Y \sim \text{uniform}(0, Mg(y))$ until $0 < r < f(y)$ Thus we have the algorithm:

Step 1: Generate $X \sim g$ and $R \sim \text{uniform}(0, 1)$

Step 2: Accept $Y = X$ if $r < \frac{f(x)}{Mg(x)}$

Step 3: Return to Step 1 otherwise.

For our situation the target density $f(x)$ is $\text{Gamma}(k, \theta)$.

We take the instrumental density $g(x)$ as $\text{Gamma}(a, b)$ where $a = [k]$ and without loss of generality we assume $\theta = 1$.

Then $M = b^{-k} \left(\frac{k-a}{(1-b)e}\right)^{k-a}$

The optimum choice of b for simulating from $\text{Gamma}(k, 1)$ is $b = \frac{a}{\alpha}$.

7. Appendix 2: Derivation of equations 6 to 10

Dividing equation (1) by equation (2),

$$\frac{dn_{Sp}}{dn_{S0}} = \frac{-2an_{Sp}^2 - n_{S0}n_{Sp}}{an_{Sp}^2 - bn_{S0}n_{Sp} - dn_{S0}^2 + en_{S0}n_{Sp}}$$

i.e.

$$dn_{Sp} = \frac{-2ax^2 - x}{ax^2 + (e-b)x - d} \left(\frac{1}{x} dn_{Sp} - \frac{n_{S0}}{x} dx \right)$$

[Since,

$$x = \frac{n_{Sp}}{n_{S0}} \text{ i.e. } dn_{Sp} = xdn_{S0} + n_{S0}dx \text{ i.e. } dn_{S0} = \frac{1}{x} dn_{Sp} - \frac{n_{S0}}{x} dx]$$

i.e.

$$\left\{1 + \frac{2ax + 1}{ax^2 + (e - b)x - d}\right\} dn_{Sp} = \left\{\frac{2ax + 1}{ax^2 + (e - b)x - d}\right\} dx \left(\frac{n_{Sp}}{x}\right)$$

i.e.

$$\frac{dn_{Sp}}{n_{Sp}} = \frac{2ax + 1}{\{ax^2 + (2a + e - b)x + (1 - d)\}x}$$

Integrating between ∞ and x and assuming at $x = \infty$, $n_{Sp} = n_0$,

$$\ln\left(\frac{n_{Sp}}{n_0}\right) = - \int_x^\infty \frac{(2ax + 1)dx}{\{ax^2 + (2a + e - b)x + (1 - d)\}x}$$

i.e.

$$\begin{aligned} \ln\left(\frac{n_{Sp}}{n_0}\right) = & - \int_x^\infty \left[\frac{1}{x} - \frac{1}{2} \left\{ \frac{2ax + (2a + e - b) + (e - b - 2a)}{ax^2 + (2a + e - b)x + (1 - d)} \right\} \right. \\ & \left. + \frac{d}{(1 - d)} \left\{ \frac{1}{x} - \frac{ax + (2a + e - b)}{ax^2 + (2a + e - b)x + (1 - d)} \right\} \right] dx \end{aligned}$$

i.e.

$$\begin{aligned} \ln\left(\frac{n_{Sp}}{n_0}\right) = & - \left[\frac{1}{2} \ln \left\{ \frac{x^2}{ax^2 + (2a + e - b)x + (1 - d)} \right\} \right. \\ & \left. + \frac{1}{2} \left(\frac{d}{1 - d} \right) \ln \frac{x^2}{ax^2 + (2a + e - b)x + (1 - d)} \right]_x^\infty \\ & - \frac{(2a + e - b)d}{(1 - d)} \int_x^\infty \frac{dx}{ax^2 + (2a + e - b)x + (1 - d)} \end{aligned}$$

i.e.

$$\begin{aligned} \ln\left(\frac{n_{Sp}}{n_0}\right) = & \ln \left\{ \frac{ax^2}{ax^2 + (2a + e - b)x + (1 - d)} \right\}^{\frac{1}{2(1-d)}} \\ & + \frac{(2a + e - b)d}{(1 - d)a\Delta} \left[\tan^{-1} \left\{ \frac{x + \frac{(2a + e - b)}{2a}}{\Delta} \right\} - \frac{\pi}{2} \right] \end{aligned}$$

where

$$\Delta^2 = \frac{1 - d}{a} - \left\{ \frac{(2a + e - b)}{2a} \right\}^2 > 0$$

otherwise Δ hence $\ln\left(\frac{n_{Sp}}{n_0}\right)$ will be imaginary.

Hence,

$$\frac{n_{Sp}}{n_0} = \left[\left\{ \frac{ax^2}{ax^2 + (2a + e - b)x + (1 - d)} \right\}^{\frac{1}{2(1-d)}} \right]$$

$$\cdot \exp\left[\frac{(2a + e - b)d}{(1 - d)a\Delta} \left(\tan^{-1}\left\{\frac{2ax + (2a + e - b)}{2a\Delta}\right\} - \frac{\pi}{2}\right)\right]$$

From equation (3)

$$dn_E = \left\{ \frac{(1 - a)x^2 + bx + cx + d}{-2ax^2 - x} \right\} \left\{ x \cdot \frac{(ax^2 - bx + ex - d)}{(1 - a)x^2 + (b + c)x + d} dn_E + \frac{n_{Sp}}{x} dx \right\}$$

i.e.

$$\left[1 + \frac{ax^2 + (e - b)x - d}{2ax + 1} \right] dn_E = - \frac{n_{Sp} \{ (1 - a)x^2 + (b + c)x + d \}}{x^2(2ax + 1)} dx$$

i.e.

$$dn_E = - \int_{\infty}^x \frac{n_{Sp} \{ (1 - a)x^2 + (b + c)x + d \}}{x^2 \{ ax^2 + (2a + e - b)x + 1 - d \}}$$

i.e.

$$dn_E = \int_x^{\infty} \frac{n_{Sp} \{ (1 - a)x^2 + (b + c)x + d \}}{x^2 \{ ax^2 + (2a + e - b)x + 1 - d \}}$$

Again dividing equation (5) by equation (1) and using

$$x = \frac{n_{Sp}}{n_{S0}}$$

$$\frac{dn_{dE}}{dn_{Sp}} = - \frac{\{k_1 a + k_2(1 - a)\}x^2 + [k_3 b + k_4 c + k_5 \{1 - (b + c + e)\}]x + dk_6 + (1 - d)k_7}{2ax^2 + x}$$

i.e.

$$dn_{dE} = - \frac{(Ax^2 + Bx + C)}{x(2ax + 1)} \left[x \frac{dn_{Sp}}{dn_{dE}} \cdot dn_{dE} + \frac{n_{Sp}}{x} \right]$$

where

$$A = k'_1 a + k'_2(1 - a)$$

$$B = k'_3 b + k'_4 c + k'_5 \{1 - (b + c + e)\}$$

$$C = dk'_6 + (1 - d)k'_7$$

Hence ,

$$dn_{dE} = - \frac{(Ax^2 + Bx + c)}{x(2ax + 1)} \left[x \frac{(ax^2 - bx + ex - d)}{(Ax^2 + Bx + c)} dn_{dE} + \frac{n_{Sp}}{x} dx \right]$$

i.e.

$$\left\{ \frac{ax^2 + (2a + e - b)x - d + 1}{(2ax + 1)} \right\} dn_{dE} = - \frac{(Ax^2 + Bx + C)n_{Sp}}{x^2(2ax + 1)} dx$$

i.e.

$$n_{dE} = \int_x^\infty \frac{(Ax^2 + Bx + C)n_{Sp}}{x^2\{ax^2 + (2a + e - b)x + (1 - d)\}} dx$$

Similarly the integral follows for n_{dIrr} . The system of equations (6) - (10) have implicit solution because each time during evaluation of the integrals (8) - (10) values of n_{Sp} are used which is a dependent variable of x .

References

- Allam, S.S., Tucker, D.L., Kent, S. et al. 2007, ASPC, 382, 261.
- Ann, H.B. 2007, in Dark Galaxies and Lost Baryons, Proceedings IAU Symposium No. 244, eds. J.I. Davies & M. J. Disney, p.346.
- Ashman, K. M., & Zepf, S. E. 1992, ApJ, 384, 50.
- Barnes, S. A., & Hernquist, L. 1992, Nature, 360, 715.
- Bergvall, N., & Johansson, L. 1985, A&A, 149, 475.
- Braine, J., Lisenfeld, U., Due, P.-A., & Leon, S. 2000, Nature, 403, 867.
- Binggeli, B., Sandage, A., & Tammann, G.A. 1985, AJ, 90, 1681.
- Binggeli, B., Tarenghi, M., & Sandage, A. 1990, A&A, 228, 42.
- Bournaud, F. & Duc, P.A. 2006, A&A, 456, 481.
- Bournaud, F. 2010, AdAst, 735284.
- Chattopadhyay, A., Chattopadhyay, T., Davoust, E., Mondal, & S., Sharina, M., 2009. ApJ 705, 1533.
- Chattopadhyay, T., Sharina, M., & Karmakar, P. 2010, ApJ, 724, 678.
- Chattopadhyay, T., Sharina, M., Davoust, E., De, T., & Chattopadhyay, A.K., 2012. ApJ 750, 91.

- Chattopadhyay, T., & Karmakar, P. 2013, *New Astronomy* 22, 22.
- Côté, P., Marzke, R. O., & West, M. J. 1998, *ApJ*, 501, 554.
- Dabringhausen J.& Kroupa P., 2013, *MNRAS* in press, arXiv:1211.1382
- Dabringhausen, J., Hilker, M.& Kroupa, P.2008, *MNRAS*.386, 864.
-] Davis, M., Peebles, P. J. E.1977,*ApJS* 34,425.
- Dekel, A., & Silk, J. 1986, *ApJ*, 303, 39.
- Delgado-Donate,E.J.,*Muôz-Turhôn* C.,Deeg,H.J. et al.2003, *A&A*, 402, 921.
- Dressler, A., Oemler, A. J., Couch, W. J. et al. 1997, *ApJ*, 490, 577.
- Dressler, A. 1980, *ApJ*, 236, 351.
- Duc, P. A., & Mirabel, I. F. 1994, *A&A*, 289, 83.
- Duc, P. A., & Mirabel, I. F. 1998, *A&A*, 333, 81.
- Duc, P.A.,Braine, J.,Lisenfeld,U. et. al. 2007, *A&A*, 473, 187.
- Dunn, J. M., 2010, *MNRAS*, 408, 392.
- Efstathiou, G.1979, *MNRAS*,187, 117.
- Ellis, R.S.,Smail, I.,Dressler,A. et al. 1997, *ApJ*, 483, 582.
- Ferguson, H. C., & Binggeli, B. 1994, *A&AR*, 6, 67.
- Ferreiro, D. L., Pastoriza, M. G., & Rickes, M. C. 2005, (arXiv:astro-ph/0510757).
- Frenk, C. S., Evrard, A. E., White, S. D. M., & Summers, F. J. 1996, *ApJ*, 472, 460.
- Forbes, D. A., Brodie, J. P., & Grillmair, C. J. 1997, *AJ*, 113, 1652.
- Ghigna, S., Moore, B., Governato, F. et al. 1998, *MNRAS*, 300, 146.
- Gott, J. R., Turner, E. L., & Aarseth, S. J.,1979, *ApJ*, 234, 13.

- Hibbard, J.E., & Higdon, J.L. 2001, ASPC, 240, 226.
- Jerjen, H., & Dressler, A.1997, A&AS, 124, 1.
- Karachentsev, I. D., Karachentseva, V. E., Huchtmeier, W. K., & Makarov, D. I. 2004, AJ, 127, 2031.
- Kauffmann, G., Nusser, A., & Steinmetz, M. 1997, MNRAS, 286, 795.
- Kaviraj, S., Darg, D., Lintott, C., Schawinski, K., & Silk, J. 2012, MNRAS, 419, 70.
- Knierman, K.A.,Gallagher, S.C.,Charlton, J.C. et al. 2003, AJ, 126, 1227.
- Kormendy, J. 1985, ApJ, 295, 73.
- Kroupa P., 2012, PASA, 29, 395433.
- Larson, R. B. 1974, MNRAS, 166, 585.
- Mateo, M. 1998, A&A, 36, 435.
- Mathews, W. G., Chomiuk, L., Brighenti, F.,& Buote, D. A. 2004, ApJ, 616, 745.
- Michard, R., & Andreon, S.2008, A&A, 490, 923.
- Mirabel, I. F., Lutz, D., & Maza, J. 1991, A&A, 243, 367.
- Mondal, S., Chattopadhyay, A.K., & Chattopadhyay, T. 2008, ApJ,683, 172.
- Mundell, Carole G., James, Phil A., Loiseau, Nora. Schinnerer, Eva, & Forbes, Duncan A. 2004, ApJ, 614, 648.
- Mendes de Oliveira, C., Plana, H., Amram, P., Balkowski, C., & Bolte, M. 2000, ASPC, 197, 253.
- Okazaki, T., & Taniguchi, Y. 2000, ApJ, 543, 149.
-]Peebles, P. J. E. 1974, ApJ, 189, 51.
- Robert, C.P. & Casella, C. 2004, in Monte Carlo Statistical Methods (Berlin: Springer), 45.

- Sandage, A., & Binggeli, B. 1984, AJ, 89, 919.
- Schweizer, F. 1982, ApJ, 252, 455.
- Shanks, T., Metcalfe, N., & Fong, D. The Extragalactic Infrared Background and its Cosmological Implications, IAU Symposium, vol 204, eds. Martin, H & Michael, G.H., p.347.
- Sheen, Y., Jeong, H., Yi, Sukyoung K. F.,
I., Lotz, J. M., Olsen, Knut A. G., Dickinson, M., Barnes, S.,
Park, J., Ree, C. H. et al. 2009, AJ, 138, 1911.
- Silk, J., & Norman, C. ApJ, 1981, 247, 59.
- Toomre, A. 1977, in The Evolution of Galaxies and Stellar
Populations, ed. B. M. Tinsley & R. B. Larson (New Haven:
Yale Univ. Press), 401.
- van Zee, L., Skillman,
E.D., & Marth, P. 2004, AJ, 128, 121.
- van Dokkum, P.G. in Tracing Cosmic Evolution with Galaxy Clusters, eds.
S. Borgani, M. Mezzetti & R. Valdarni (San Fransisco: ASP), 265.
- White, S. D. M., & Frenk, C. S. 1991, ApJ, 379, 52.
- Weilbacher, P. M., Duc, P. -A., Fritze-v.Alvensleben, U., Martin,
P., & Fricke, K. J. 2000, A&A, in press (astro-ph/0004405).
- White, S. D. M. & Rees, M. J. 1978, MNRAS, 183, 341.
- Yahil, A., Lanzetta, K. M., & Fernandez-Soto, A.
1998, arXiv:astro-ph/9803049.
- Yoshida, M., Taniguchi, Y., & Murayama, T. 1994, PASJ, 46, L195.
- Zepf, S. E., Beasley, M. A., Bridges, T. J., Hanes, D. A.,
Sharples, R. M., Ashman, K. M., & Geisler, D. 2000, AJ, 120,
2928.

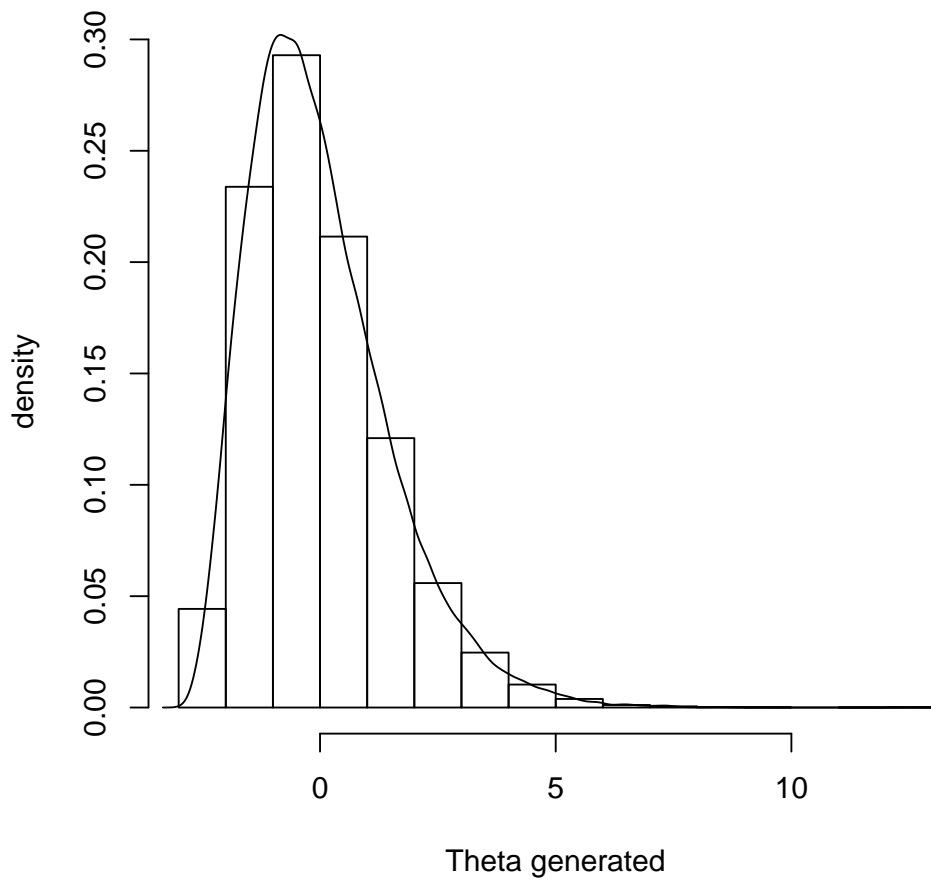


Figure 1: The generated values of Θ from Gamma distribution.

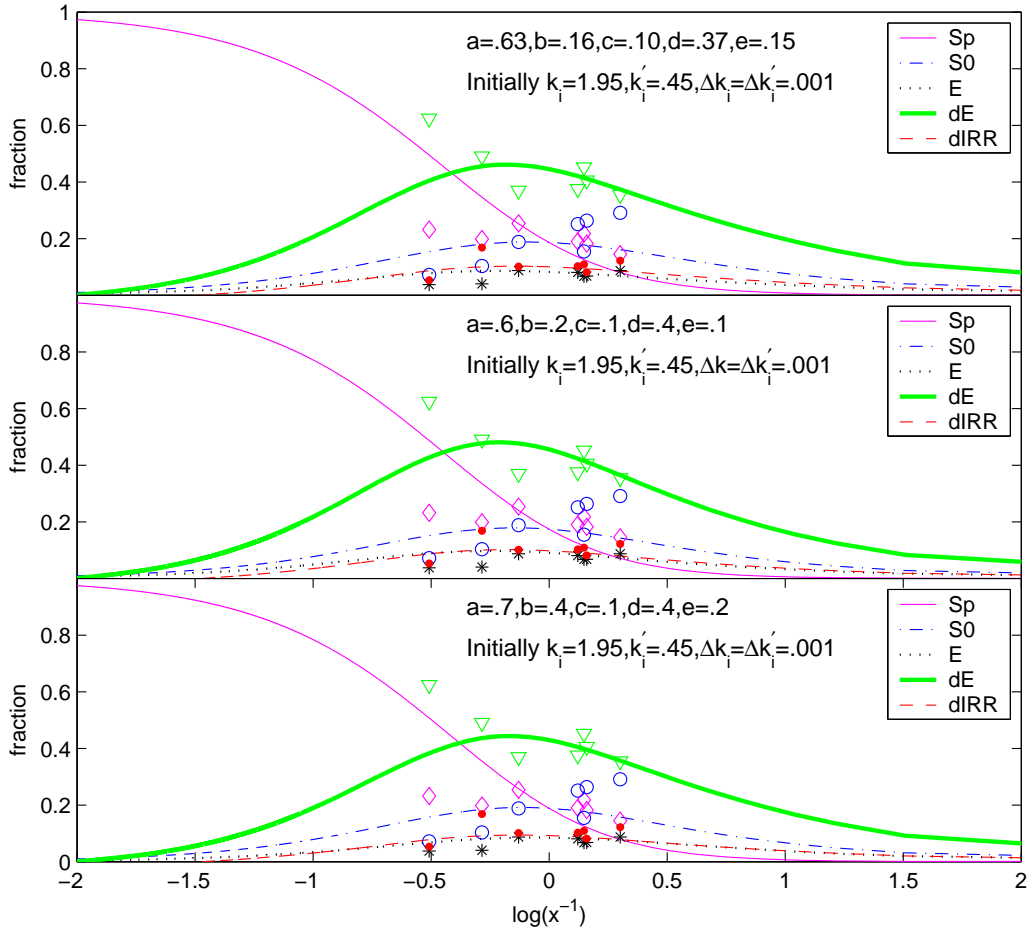


Figure 2: Simulated values of the fractions of galaxies of various morphological types with observed values for some of the values of impact parameters as a function of $\log(1/x)$. Magenta open diamonds are for Spiral galaxies, blue open circles are for S0 galaxies, black stars are for Ellipticals, green open triangles are for dEs and red solid circles are for dIRrs.

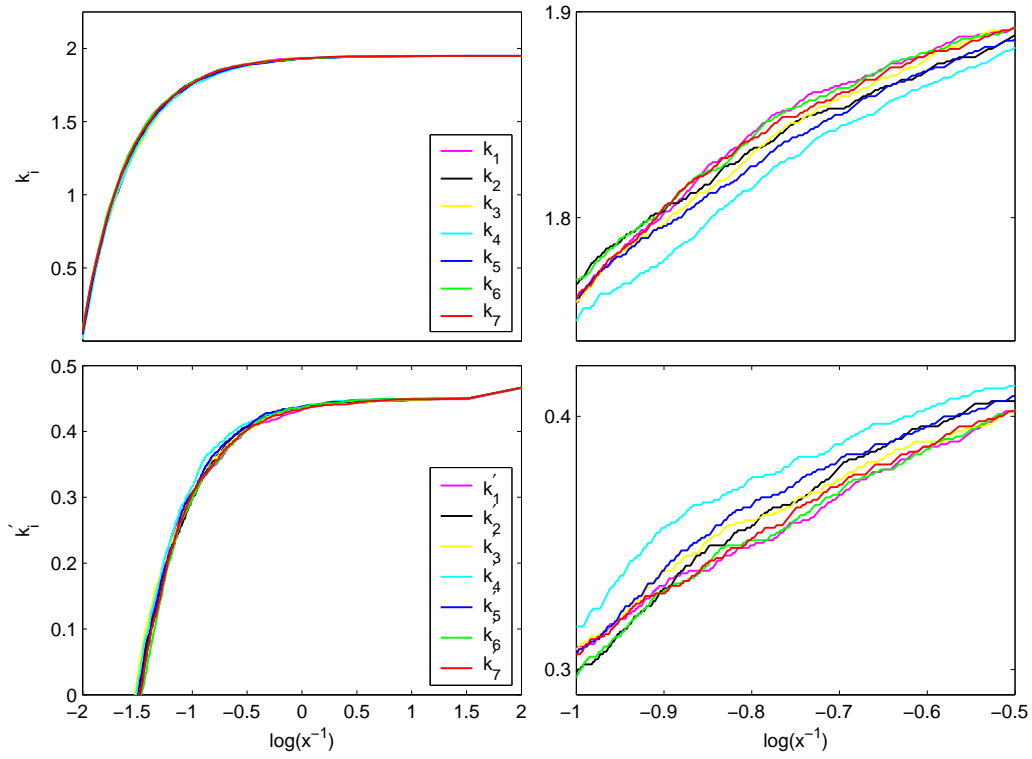


Figure 3: Simulated values for k_i , the number of dEs formed, and k'_i , the number of dIrrs formed, ($i=1-7$), as a function of space density.

Table 1: Observed values of Θ used from Karachentsev et al.(2004) in Chattopadhyay et al.(2010)

Galaxy names	Θ	T	Galaxy names	Θ	T
E349-031	0.5	10	UGC7242	0.4	10
E410-005	0.4	-1	DDO113	1.6	10
E294-010	1.0	-3	DDO125	-0.9	10
KDG2	0.4	-1	UGC7605	0.7	10
E540-032	0.6	-3	E381-018	-0.6	10
UGC685	-1.6	9	E443-09	-0.9	10
KKH5	-1.2	10	KK182	1.2	10
KKH6	-0.8	10	UGC8215	-0.5	10
KK16	-0.4	10	E269-58	1.9	10
KK17	-0.3	10	KK189	2.0	-3
KKH34	-0.8	10	E269-66	1.7	-1
E121-20	-1.6	10	KK196	2.2	10
E489-56	-2.1	10	KK197	3.0	-3
KKH37	-0.3	10	KKs55	3.1	-3
UGC3755	-2.1	10	14247	1.5	10
E059-01	-1.5	9	UGC8508	-1.0	10
KK65	-2.0	10	E444-78	2.1	10
UGC4115	-1.7	10	UGC8638	-1.3	10
DDO52	-1.5	10	KKs57	1.8	-3
D564-08	-1.9	10	KK211	1.5	-5
D565-06	-1.8	10	KK213	1.7	-3
KDG61	3.9	-1	KK217	1.1	-3
KKH57	0.7	-3	CenN	0.9	-3
HS117	1.9	10	KKH86	-1.5	10
UGC6541	-0.7	10	UGC8833	-1.4	10
NGC3741	-0.8	10	E384-016	0.3	10
E320-14	-1.2	10	KK230	-1.0	10
KK109	-0.6	10	DDO190	-1.3	10
E379-07	-1.3	10	E223-09	-0.8	10
NGC4163	0.1	10	IC4662	-0.9	9

Table 2: Merger scheme

Serial no.	Galaxy type	Probability	Galaxy formed
1	Sp + Sp \rightarrow	(a)	S0 + k_1 dE / k'_1 dIrr
		(1-a)	E + k_2 dE / k'_2 dIrr
2	Sp + S0 \rightarrow	(b)	E + k_3 dE / k'_3 dIrr
		(c)	E + S0 + k_4 dE / k'_4 dIrr
		(e)	S0 + S0 + k_8 dE / k'_8 dIrr
		1 - (b+c+e)	S0 + k_5 dE / k'_5 dIrr
3	S0 + S0 \rightarrow	(d)	E + k_6 dE / k'_6 dIrr
		(1-d)	S0 + S0 + k_7 dE / k'_7 dIrr

Table 3: Observational numbers of galaxies of various morphological types in clusters of galaxies.

Data set	Cluster	E	S0	Sp	dE	dIrr	x	$\log(1/x)$
1	Virgo	20	53	102	252	87	1.92	-0.284
	Coma0	37	115	87	172	47	0.7565	0.12118
	Coma1	15	50	25	61	21	0.5	0.30103
	Coma2	10	39	27	60	12	0.69	0.1597
	Coma3	12	26	35	51	14	1.3461	-0.12909
2	Centaurus	16	37	52	108	26	0.7838	0.1478
3	VirgoII	60	114	367	960	82	3.21	-0.5078

Table 4: Best fit Chisquare estimates and corresponding ranges of parameters

a	b	c	d	e	$k_i (i=1-7)$ Fig. 3	$k_i (i=1-7)$ Fig. 3	χ^2 0.9 ± 0.15	p-value 0.995
0.55 - 0.80	0.10 - 0.55	0.05 - 0.70	0.35 - 0.40	0.05 - 0.40				

Table 5: Observed number of dwarf galaxies in individual galaxy mergers

HII Regions of TDG cadidates	Number	Reference
1	12	Ferreiro et al. 2005
2	11	
3	7	
4	4	
5	4	
6	4	
7	5	
8	3	
9	3	
10	2	
11	1	
Stephan's quintet	5	Oliverira et al. 2000
NGC4922	3	Sheen et al. 2009
NGC4038/9	2	Hibberd & Higdon 2001
NGC3227/3226	1	Mundell et al. 2004
NGC7252	2	Schweizer 1982
ESO 148 - IG02	3	Bergvall & Johansson 1985
The Superantennae NGC4038/4039	9	Mirabel et al.1991
Arp 105	2	Duc & Mirabel 1994
NGC2782	1	Yoshida et al. 1994
NGC5291	11	Duc & Mirabel 1998